Journal of the Korean Chemical Society
2023, *Vol. 67, No. 4*
Printed in the Republic of Korea
https://doi.org/10.5012/jkcs.2023.67.4.217

Spectrophotometric Determination of Maximum Loading Capacity of a Dendrimer

Youngjin Jeon
Department of Applied Chemistry, College of Science and Technology, Konkuk University, Chungju 27478, Korea.
E-mail: jeonyj@kku.ac.kr
(Received April 18, 2023; Accepted June 13, 2023)

ABSTRACT. A series of hydrophobic dodecyl-terminated 6th-generation poly(amidoamine) dendrimer (**H**)-encapsulated cadmium sulfide ($(CdS)_n$@**H**) nanoparticles in a co-solvent (toluene: methanol = 6.8: 3.2 v/v) are synthesized. The diameters of CdS nanoparticles within the dendrimer were estimated by analyzing the positions of the first excitonic absorption peaks of CdS in UV-vis spectra. The size of the CdS nanoparticle within the dendrimer shows a saturation value as the CdS/**H** ratio (n) increases, which is believed to be due to the limited physical size of the void cavity within the dendrimer. This simple and convenient method of estimating the saturation of the size of CdS in dendrimers may be useful in determining the maximum void space within other dendrimers under various solvent conditions.

Key words: Cadmium sulfide, Dendrimer, UV-vis spectra, Maximum loading capacity, Nanoparticles

INTRODUCTION

Dendrimers are monodisperse spherical macromolecules with a repeating, branched unit structure featuring a multifunctional core with a high density and precise functional groups attached to the outer surface.[1] Since the pioneering synthesis of dendrimers by Tomalia,[2] different types of dendrimers have been synthesized and found numerous useful applications, mainly as hosts for drugs,[3] metal nanoparticles,[4] semiconductor nanomaterials,[5] catalysts,[6] and bioimaging.[7] Dendrimers can also serve as stabilizers for metal or semiconductor nanoparticles.[8] Many guest molecules have been introduced into void space inside dendrimers. The void space inside dendrimers can vary depending on the type of dendrimer, generation, and solvent conditions. Many researchers have endeavored to understand the behavior of dendrimers in solutions using molecular dynamics, SAXS, and SANS techniques.[9] However, they provided the size of dendrimers that are variant depending on the pH of the solution and elucidated the size of the internal cavity of dendrimers indirectly.[10] The comprehension of the maximum internal capacity for hosting a guest molecule through experimental endeavors is significantly limited. A research group reported on the maximum loading capacity of Cu nanoparticles in a poly(amidoamines) (PAMAMs) dendrimer. They found the diameter of Cu_{57} nanoparticles sequestered in a hydroxy-terminated PAMAMs (G6-OH) dendrimer approximately 2.6 nm, which is in severe disagreement with the theoretical size of Cu_{57} nanoparticles (1.1 nm).[11]

Dendrimers often employ semiconductor materials as guest molecules. Cadmium sulfide (CdS) is popular due to its direct band gap II-VI semiconductor properties at room temperature, characterized by an E_g value of 2.4 eV.[12] The synthesis of dendrimer-encapsulated CdS nanoparticles,[13] with a size range of 1-2 nm, is straightforward compared to alternative methods. Cd^{2+} ions are typically loaded into a dendrimer, followed by the addition of sulfide ions, resulting in CdS nanoparticles with varying sizes. The size-dependent optical properties of CdS make it a suitable guest molecule for many studies, where it can be used to determine the size of CdS nanoparticles generated within dendrimers. Although transmission electron microscopy (TEM) is a precise method for evaluating the size of nanometer-scale structures, more is needed for quickly measuring multiple samples in routine testing.[14] To address this issue, alternative approaches that estimate the size of nanoparticles based on optical absorption measurements have been developed.[15] These methods depend on determining the edge of the absorption band, which is influenced by the diameter of the nanocrystal. However, estimating their sizes using these methods can be challenging in cases where nanoparticles with different sizes are mixed.

Herein, we report a convenient method to measure the practical maximum loading capacity (or size of void space) of a dendrimer by the synthesis of a series of 6th-generation hydrophobic dendrimer(**H**)-encapsulated CdS nanoparticles ($(CdS)_n$@**H**) in a co-solvent system composed of tol-

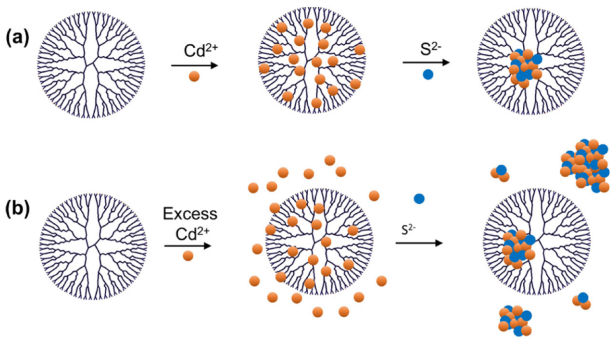

***Scheme* 1.** Schematic diagram of (a) the formation of dendrimer-encapsulated CdS nanoparticles within the capacity of void space inside a dendrimer and (b) the formation of CdS particles inside as well as outside a dendrimer when the size of CdS particles exceeds the capacity of void space of the dendrimer.

uene and methanol (6.8:3.2 v/v). The size of the CdS particles is controlled by the molar ratio of Cd^{2+} and S^{2-} to **H**. The diameter of the nanoparticles is determined by analyzing the wavelength of the first excitonic absorption peaks of CdS nanoparticles in UV-vis spectra of corresponding assemblies. This simple method offers a facile method for determining the maximum guest size that could be accommodated inside a dendrimer depending on the kind of dendrimers and solvents.

EXPERIMENTAL

All the chemicals were purchased from commercial sources, which include cadmium nitrate tetrahydrate ($Cd(NO_3)_2 \cdot 4H_2O$, 99.0%, Sigma-Aldrich, USA), sodium sulfide (Na_2S, 99.9%, Sigma-Aldrich, USA), and dodecyl-terminated 6th generation PAMAM Dendrimer G6-50% C12 Hydrophobic (Sigma-Aldrich, USA).

Preparation of ((CdS)$_n$/H))

The synthetic procedure has been modified from the common synthetic method of dendrimer-encapsulated CdS nanoparticles.[13] Briefly, the stock solutions of dodecyl-terminated 6th-generation PAMAM dendrimer **H** (0.50 mM) in toluene, $Cd(NO_3)_2$ (20 mM) in methanol, and Na_2S (20 mM) in methanol was prepared and used as the reactants. The designated amount of the stock solutions in *Table* S1 of **H** and Cd^{2+} were mixed first to form a complex of Cd^{2+} with the tertiary amines inside the dendrimer and agitated for 10 min. Subsequently, the stock solution of Na_2S was injected to form dendrimer-encapsulated CdS in the solution (toluene:MeOH = 6.8:3.2 v/v). The final volume of the solution is fixed at 10 mL. A series of (CdS)$_n$@**H**, in which molar ratios (n) of CdS/**H** are 16, 64, and 254. And for the saturation test, **1**-**10** samples were prepared, in which the molar ratios of CdS/**H** were 16 for **1**, 40 for **2**, 64 for **3**, 160 for **4**, 254 for **5**, 400 for **6**, 500 for **7**, 700 for **8**, 960 for **9**, and 1200 for **10**, respectively.

Characterization

UV-vis spectra were recorded on a photodiode array Agilent 8453 UV-vis spectrophotometer (Agilent, Inc., USA) and 1.00 cm quartz cuvettes. All spectra were background-corrected using a spectrum obtained from solvent (toluene:MeOH = 6.8:3.2 v/v). Photoluminescence (PL) spectra were obtained using a Fluorolog Spectrofluorometer (Horiba Jobin Yvon, Germany) and 1.0 cm quartz cuvettes. After preparing the samples, 3 mL of the resulting solution was transferred to a 1.0 cm-thick quartz cuvette and used for UV-vis and PL spectra acquisition. Detailed information for the concentration and volume of the reactant solutions and solvents are provided in Table S1 in the Supporting Information. Scanning electron microscopic (SEM) images and energy-dispersive X-ray spectra (EDS) were obtained using a JEOL JSM-7610F field emission scanning electron microscope (Japan). High-resolution transmission electron microscopic images were obtained using a JEOL model JEM 2010 microscope at an acceleration voltage of 200 kV.

RESULTS AND DISCUSSION

As a preliminary study, the formation of size-monodisperse CdS inside a hydrophobic 6th-generation dodecyl-terminated poly(amidoamine) dendrimer (**H**) was evaluated. Half of the outer surface terminal groups of **H** are decorated with dodecyl groups, while the rest of the end groups remain amines. In this preparation, **H** acts as a nanoreactor and an internal stabilizer for forming the CdS nanoparticles. For this purpose, three **H**-encapsulated CdS nanoparticles ((CdS)$_n$@**H**), with molar ratios (n), CdS/**H** of 16, 64, and 254, were synthesized by the experimental procedure described in the Experimental section and *Table* S1. Briefly, CdS nanoparticles were synthesized within **H** using the following method: First, Cd^{2+} ions were sequestered within **H** simply by mixing a $Cd(NO_3)_2$ solution with an **H** solution for 10 min. The main driving force for the sequestration of Cd^{2+} ions in the dendrimer is known to be the solubility difference of Cd^{2+} ions in solvent and the interior of the dendrimer and coordination of Cd^{2+} to tertiary amines of the dendrimer.[13] Then, a rapid injection of Na_2S solution led to the formation of CdS nanoparticles within

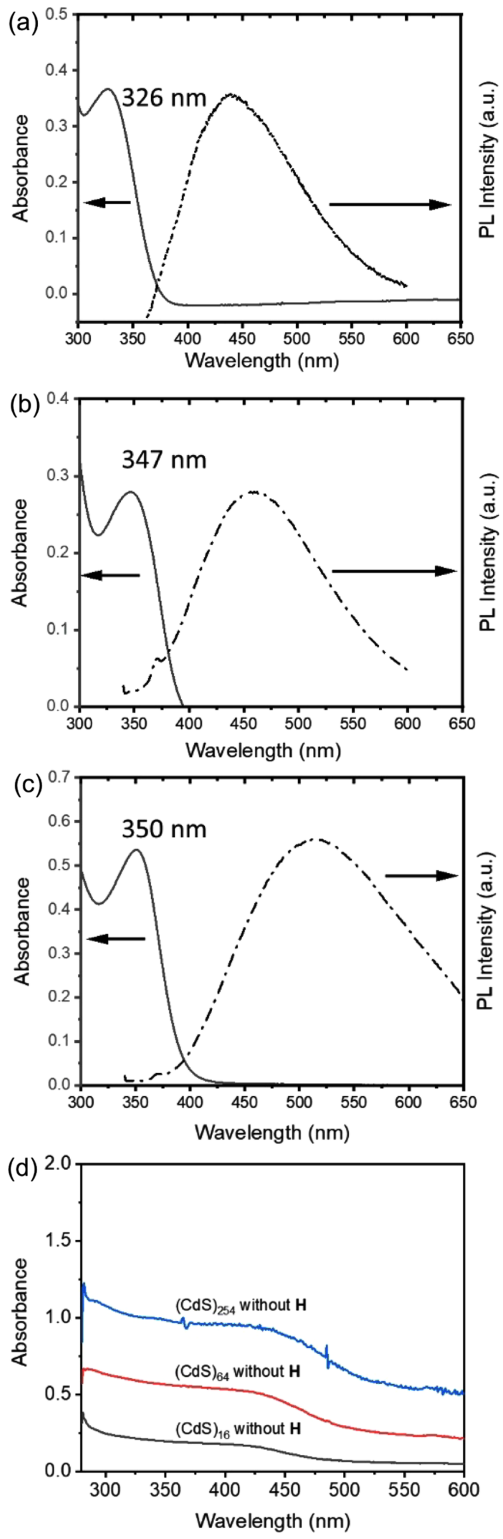

***Figure* 1.** UV-vis and PL spectra of CdS nanoparticles of (a) CdS/**H** = 16:1, (b) 64:1, and (c) 254:1. Each PL spectrum (right) was obtained by excitation at first absorption peaks of corresponding UV-vis spectrum (left). (d) UV-vis spectra of CdS nanoparticles by the same experimental condition as in (a)-(c), but in the absence of **H**.

the dendrimer. As shown in *Fig.* 1, $(CdS)_{16}$@**H**, $(CdS)_{64}$@**H**, and $(CdS)_{254}$@**H** have the first absorption peak positions at 326 nm, 347 nm, and 350 nm, respectively. Excitation photoluminescence (PL) spectra were recorded by excitation on the first absorption peak of the UV-vis spectra of corresponding samples. The excitations at first excitonic absorption peaks produce the PL excitation peaks at 439 nm, 460 nm, and 514 nm, respectively.

To clarify the formation of CdS nanoparticles inside **H**, the same experiments in the absence of **H** were performed. As shown in *Fig.* 1(d), CdS was synthesized without specific peaks over the full span of the spectra. This result confirms that the size-monodisperse CdS in $(CdS)_n$@**H** assemblies could be synthesized within the dendrimer.

Transmission electron microscopy (TEM) is a commonly used method for evaluating the size of nanoparticles. TEM provides precise measurements of the shape and size of nanometer-scale structures.[14] In this study, poor electron beam absorption of Cd^{2+} in TEM forced us to choose methods other than TEM to evaluate the above particle sizes ranging from 1~2 nm. Among them,[15] Yu *et al.* reported that the average particle size of CdS could be estimated by the wavelengths of the first absorption peaks in the UV-vis spectra of CdS by the following empirical formula as shown below:[16]

$$D = (-6.6521 \times 10^{-8})\,\lambda^3 + (1.9557 \times 10^{-4})\,\lambda^2 - (9.2352 \times 10^{-2})\,\lambda + (13.29)$$

where D (nm) is the diameter of a CdS nanoparticle, and l (in nm) is the wavelength of the first excitonic absorption peak of the corresponding sample. It should be noted that the formula provided above is only polynomial fitting functions of the experimental data, which may need to be revised in size ranges not covered by the data in the 1.5~5.6 nm range. Average particle sizes obtained by Yu's empirical formula for $(CdS)_{16}$@**H**, $(CdS)_{64}$@**H**, and $(CdS)_{254}$@**H** are 1.68 nm, 1.99 nm, and 2.07 nm, respectively. Theoretical calculations of particle sizes for the corresponding CdS, based on the molar volumes (V_m) of Cd and S, reveal distinct differences. Specifically, the Theoretical diameters for $(CdS)_{16}$@**H**, $(Cd)_{64}$@**H**, and $(CdS)_{254}$@**H** are 1.13 nm, 1.80 nm, and 2.84 nm, respectively. Yu's empirical formula does not cover the size of $(CdS)_{16}$@**H**, while $(CdS)_{64}$@**H** displays a close coincidence between the two values. However, a notable discrepancy is observed between the sizes of $(CdS)_{254}$@**H** calculated by Yu's formula and its corresponding theoretical value. These observations underscore the need to investigate the maximum particle size of CdS nanoparticles that the host

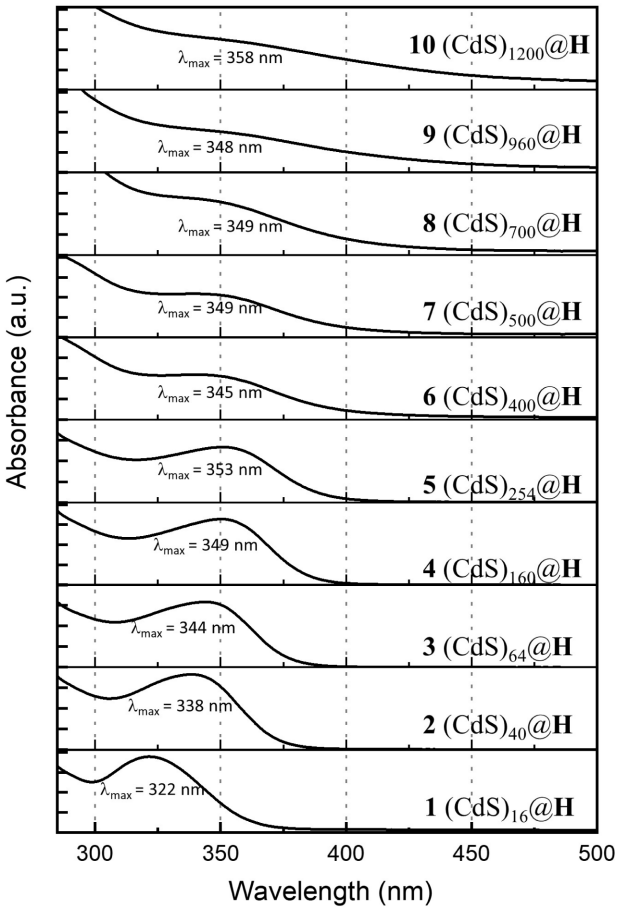

***Figure* 2.** UV-vis absorption spectra of the samples: **1**: $(CdS)_{16}$@**H**; **2**: $(CdS)_{40}$@**H**; **3**: $(CdS)_{64}$@**H**; **4**: $(CdS)_{160}$@**H**; **5**: $(CdS)_{254}$@**H**; **6**: $(CdS)_{400}$@**H**; **7**: $(CdS)_{500}$@**H**; **8**: $(CdS)_{700}$@**H**; **9**: $(CdS)_{960}$@**H**; **10**: $(CdS)_{1200}$@**H**, from bottom to top, respectively. The positions of the first absorption peaks were denoted as λ_{max}.

can accommodate.

To study the effect of CdS/**H** ratios (n) on UV-vis spectra, a series of $(CdS)_n$@**H** samples with different values of n were prepared. The samples (**1-10**) had n values of 16, 40, 64, 160, 254, 400, 500, 700, 960, and 1200, respectively. Sample **1** displayed a first absorption peak at 322 nm, while sample **2** had one at 338 nm and sample **3** at 344 nm, as shown in *Fig*. 2. Sample **4** reached a saturation point in the increase of the position of the first absorption peak. In contrast, samples **5** to **10** were unable to identify the exact positions of the first absorption peaks due to the blurred peaks in the spectra.

Therefore, deconvolution was necessary to distinguish the first absorption peaks from CdS formed inside **H** from the absorption of CdS outside **H**. Figure S1 displays the deconvolution of the spectra of samples **5-10**. No further increase was seen in samples **5** to **10**, potentially owing to

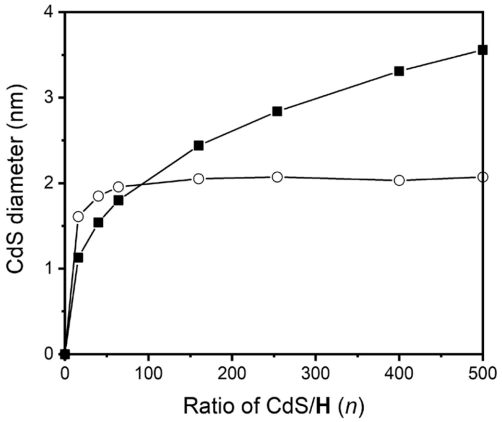

***Figure* 3.** The trend in diameters of CdS nanoparticles in $(CdS)_n$@**H** as a function of CdS/**H** ratio (n) calculated by *Yu*'s formula from the UV-vis spectra (open circles) and theoretical diameters of $(CdS)_n$ calculated based on the molar volume (V_m) of Cd and S under the assumption that the internal void cavity of the dendrimer is not limited (closed squares).

the limited size of the void space within **H**. As revealed by the deconvoluted spectra, the gradual saturation in the position of absorption indicates CdS formation outside of **H**. This results in a broad size distribution ranging from sub-nanometer to significantly larger than the CdS formed inside **H**. These results confirm that CdS nanoparticles larger than a specific size could not fit inside the dendrimer and therefore were generated outside.

The relationship between the CdS/**H** ratio (n) and the diameter of CdS nanoparticles within the dendrimer is demonstrated in *Fig*. 3. The data indicate that the size of CdS inside the dendrimer is saturated due to the limited capacity of the internal void cavity of the dendrimer. Based on Yu's empirical formula, the estimated average diameter of CdS in samples **5-10** is 2.04 ± 0.05 nm, corresponding to approximately $(CdS)_{60}$. The theoretical particle sizes of CdS in $(CdS)_n$ were calculated and shown in *Fig*. 3 (filled squares). It displays the theoretical sizes of $(CdS)_n$@**H** for the respective samples, which deviate from the values calculated using Yu's formula for samples **5-10** (open circles). This suggests that the physical void space of **H** constrains the size of CdS nanoparticles sequestered within it.

Fig. S2 displays high-resolution transmission electron microscopic (HR-TEM) images and X-ray energy dispersive spectroscopic (EDS) data of **1** and **10**. The HR-TEM image of sample **1** in *Fig*. S2 shows its transparency under HR-TEM imaging. Therefore, the detection of CdS nanoparticles can be challenging. Still, their presence is confirmed through EDS data, which reveals an atomic ratio of Cd to S close to 1:1. In contrast to sample **1**, sample **10** demonstrates

a notable aggregation of CdS nanoparticles that have formed outside of **H** and are larger than 2 nm in size. *Fig*. S3 shows the EDS result of sample **10**, which also supports the severely aggregated entities are CdS.

CONCLUSION

In this study, a series of hydrophobic poly(amidoamine) dendrimer (PAMAM)-encapsulated cadmium sulfide ((CdS)n@**H**) using a co-solvent (toluene: methanol = 6.8: 3.2 v/v) system were synthesized. The size of the CdS formed inside the dendrimer is determined by the molar ratio of Cd^{2+} and S^{2-} to **H**. The diameters of a series of $(CdS)_n$ were estimated by the positions of the first absorption peaks of CdS in UV-vis spectra and exhibited a saturation to a specific value as *n* increases, likely due to the limited size of the void cavity inside the dendrimer. These results offer insight into the effective void cavity size for guest molecule accommodation in a dendrimer. The method herein might be applied to determine the maximum loading capacity of other dendrimers. It might have promising implications for various research areas and offers essential information such as drug delivery.

Acknowledgments. Publication cost of this paper was supported by the Korean Chemical Society.

Supporting Information. Detailed information of reactants for product formation, deconvolution data for sample **1-10**, and HR-TEM images and EDS data for **1** and **10** are available online.

REFERENCES

1. (a) F. Vögtle, Ed. *Dendrimers Topics in Current Chemistry*; Springer: New York, 1998. (b) Alper, J. *Science* **1991**, *251*, 1562. (c) Newkome, G. R.; Yao, Z. Q.; Baker, G. R.; Gupta, V. K.; Russo, P. S.; Saunders, M. J. *J. Am. Chem. Soc.* **1986**, *108*, 849.
2. (a) Tomalia, D. A.; Baker, H.; Dewald, J.; Hall, M.; Kallos, G.; Martin, S.; Roeck, J.; Ryder, J.; Smith, P. *Polym. J.* **1985**, *17*, 117. (b) Tomalia, D. A.; Fréchét, J. M. J. *J. Polym. Sci.* **2002**, *40*, 2719. (c) Esfand, R.; Tomalia D. A. *Drug Discov. Today* **2001**, *6*, 427.
3. (a) Medina, S. H.; El-Sayed, M. E. H. *Chem. Rev.* **2009**, *109*, 3141. (b) Wang, J.; Li, B.; Qiu, L.; Qiao, X.; Yang, H. *J. Biol. Eng.* **2022**, *16*, 18. (c) Patri, A. K.; Kukowska-Latallo, J. F.; Baker, J. R. *Adv. Drug Deliv. Rev.* **2005**, *57*, 2203. (b) Tomalia, D. A.; Nixo, L. S.; Hedstrand, D. M. *Biomolecules* **2020**, *10*, 642.
4. (a) Bronstein, L. M.; Shifrina, Z. B. *Chem. Rev.* **2011**, *111*, 5301. (b) Barman, S. R.; Nain, A.; Jain, S.; Punjabi, N.; Mukherji, S.; Satija, J. *J. Mater. Chem. B* **2018**, *6*, 2368.
5. (a) Mondal, S.; Ghosh, D.; Roy, C. N.; Saha, A. *RSC Adv.* **2014**, *4*, 13085. (b) Chaput, J. C.; Switzer, C. *J. Am. Chem. Soc.* **2000**, *122*, 12886.
6. (a) Liu, X.; Gregurec, D.; Irigoyen, J.; Martinez, A.; Moya, S.; Ciganda, R.; Hermange, P.; Ruiz, J.; Astruc, D. *Nat. Commun.* **2016**, *7*, 13152. (b) Yamamoto, K.; Imaoka, T.; Tanabe, M.; Kambe, T. *Chem. Rev.* **2020**, *120*, 1397. (c) Niu, Y.; Crooks, R. M. *C. R. Chim.* **2003**, *6*, 1049.
7. (a) Barrett, T.; Ravizzini, G.; Choyke, P. L.; Kobayashi, H. *IEEE Eng. Med. Biol. Mag.* **2009**, *28*, 12. (b) Caminade, A.-M.; Hameau, A.; Turrin, C.-O.; Laurent, R.; Majoral, J.-P. *Coord. Chem. Rev.* **2021**, *430*, 213739.
8. (a) Wu, X. C.; Bittner, A. M.; Kern, K. *J. Phys. Chem. B* **2005**, *109*, 230. (b) Deraedt, C.; Ye, R.; Ralston, W. T.; Toste, F. D.; Somorjai, G. A. *J. Am. Chem. Soc.* **2017**, *139*, 18084.
9. (a) Maiti, P. K.; Cuagin, T.; Lin, S.-T.; Goddard, W. A. *Macromolecules* **2005**, *38*, 979. (b) Markelov, D. A.; Semisalova, A. S.; Mazo, M. A. *Macromol Chem Phys* **2021**, *222*, 2100085.
10. Topp, A.; Bauer, B. J.; Tomalia, D. A.; Amis, E. J. *Macromolecules* **1999**, *32*, 7232.
11. Patala, R.; Noh, J.-H.; Meijboom, R. *Int. J. Chem. Kinet.* **2018**, *50*, 693.
12. Lee, M.; Han, S.; Jeon, Y. J. *Bull. Korean Chem. Soc.* **2010**, *31*, 3818.
13. (a) Lemon, B. I.; Crooks, R. M. *J. Am. Chem. Soc.* **2000**, *122*, 12886. (b) Méndez, P. F.; Sepulveda, S.; Manríquez, J.; Rodríguez, F.J.; Bustos, E.; Rodríguez, A.; Godínez, L. A. *J. Cryst. Growth* **2012**, *361*, 108.
14. Jeon, Y.; Choi, K.; Lee, S.; Heo, J. *Bull. Korean Chem. Soc.* **2021**, *42*, 889.
15. Rodríguez-Mas, F.; Ferrer, J. C.; Alonso, J. L.; Valiente, D.; de Ávila. S. F. *Crystals* **2020**, *10*, 226.
16. (a) Yu, W. W.; Qu, L.; Guo, W.; Peng, X. *Chem. Mater.* **2003**, *15*, 2854. (b) Vossmeyer, T.; Katsikas, L.; Giersig, M.; Popovic, I. G.; Diesner, K.; Chemseddine, A.; Eychmuller, A.; Weller, H. *J. Phys. Chem.* **1994**, *98*, 7665.